이학석사 학위논문

LCST 행동에 영향을 미치는 PDMA의 건축 변경

Architectural change of poly (*N*,*N*- dimethylacrylamide) affecting on the LCST behavior

울산대학교 대학원

화 학 과

아시에 도안

Architectural change of poly (*N*,*N*-dimethylacrylamide) affecting on the LCST behavior

지도교수 이 형 일

이 논문을 이학석사학위 논문으로 제출함

2022년 02월

울산대학교 대학원

화학과

아시예 도안

아시예 도안의 석사학위 논문을
인준함

심사위원 이형일 인

심사위원 이승구 인

심사위원 김범진 인

울산대학교 대학원
2022년 02월

Contents

Abstract

A series of poly(dimethylacrylamide) (PDMA) bottlebrushes with various side chain length tailoring on the backbone were synthesized by the “grafting-from” approach using reversible addition-fragmentation chain transfer polymerization (RAFT). ATRP was employed to synthesize poly(2-hydroxyethyl methacrylate) (PHEMA) with high molecular weight (degree of polymerization, DP = 500) , followed by reacting with EMP to yield $PHEMA_{500}$-EMP as a macro-CTA (backbone). *N,N*-dimethylacrylamide (DMA) was grafted from macro-CTA to yield a series of bottlebrushes ($PHEMA_{500}$-EMP-*g*-PDMA) with various side chain lengths. Bottlebrushes were characterized by gel permeation chromatography (GPC) and ^{1}H NMR. The molecular weight distribution was low ($M_w/M_n = 1.2$-1.3). Transmittance spectra of the aqueous solutions of linear homopolymer and bottlebrush polymer of PDMA at 650 nm were measured by Uv-vis for comparing the effect of change in architecture on LCST behavior of PDMA with the same degree of polymerization. The results demonstrate that PDMA is dramatically affected by changes in architecture and PDMA bottlebrushes exhibited LCST below 100 ^{o}C.

Keywords:

Poly(dimethyacrylamide) (PDMA); polymer-polymer interaction; polymer architecture; reversible addition-fragmentation chain transfer (RAFT); bottlebrush; LCST.

1. Introduction

The architecture of polymers greatly affects the properties of the polymer. The architecture of interest is bottlebrush polymers are with long, densely grafted linear side chains on a linear backbone, mostly known as bottlebrush polymers, have unique properties that attracted great attention in various fields.[1-6] Bottlebrushes are chemically attached to the flexible backbone with the linear side chains separated by a distance much smaller than their unperturbed dimensions, bottlebrushes show extraordinary rheological properties, connected to a shift of entanglement molecular weight to higher values, which are the main focus of research so far.[7-10]

Moreover, the properties of polymer brushes are controlled by changes in the length of the side chains in the grafting density.[1,12] Brush polymers have been synthesized by three methods: grafting-onto,[39] grafting-through,[40-42] and grafting-from.[43-45] The grafting-from method has been broadly studied due to its ability to synthesize brushes with high grafting density from a backbone.

In the last two decades, thermoresponsive polymers showing phase transition at low critical solution temperature (LCST) occupy a large space in polymer science.[13-17] The decrease of polymer solubility with increasing temperature is a kind of thermo-responsive polymer and known to exhibit a well-known lower critical solution temperature (LCST).[18] The process of LCST is that the polymer chains precipitated and dehydrated at temperatures above the LCST, and completely dissolved and hydrated at temperatures below the LCST.[24] One of the best known thermo-responsive polymer is poly(N isopropylacrylamide) PNIPAM which displays a LCST in the water around 32 °C, has been the most studied thermoresponsive polymer due to its LCST being close to body temperature.[17,19-23] Generally, the smart response in thermo-responsive polymers is frequently realized by copolymerizing N,N-dimethylacrylamide (DMA) with stimuli-responsive macromolecules.[25-28] The lower critical solution temperature (LCST) of PDMA, whose phase-transition temperature in pure water is far higher than the usual critical temperature range (5–100 ºC) for smart polymers. According to previous studies, LCST for PDMA was previously estimated to be above 200 ºC.[25-28] Interestingly, LCST of PDMA is the highest phase-transition temperature among all poly(N,N-dialkylacrylamide)s.

In the literature, it has been reported that the LCST of the polymers can be controlled by a variety of methods. One of the most interesting method is the preparation of thermo-responsive polymers by copolymerization with hydrophilic and hydrophobic comonomers.[30-33] Furthermore, the addition of salts[34] and/or surfactants,[35] pH,[36] and organic solvent[37,38] to the polymer solution was also found to be an effective method to control LCST behavior (Scheme 1).

More specifically, interactions that lead to attraction between polymer-water and polymer-polymer are the dominant factors for the determination of LCST behavior. Structural factors that enhance the polymer-water interactions result in increase in LCST. However on the contrary, increment in the polymer-polymer interactions decreases the value of LCST. Further, LCST transition mainly is driven by the effect of entropy which is determined by the change of configuration numbers of water molecules, while the latter originate mainly from the enthalpic interaction between polymers, such as ionic and hydrogen bonding, which changes more gradually. Based on these hypotheses, we report the LCST of PDMA can be controlled by the effect of the change in the polymer architecture on the LCST value of the PDMA which is unlike the method in the literature. For this purpose, we synthesized PDMA bottlebrushes that were different side chain lengths, high molecular weight, and relatively low polydispersities using grafting-from approach by RAFT.

2. Experimental

2.1 Materials

2-Hydroxyethyl methacrylate (HEMA, TCI), and *N,N*-dimethylacrylamide (DMA, TCI, 99.0%) were purified by passing through a column filled with basic alumina before the polymerization to remove inhibitors. 2,2'-Azobis(isobutyronitrile) (AIBN, Sigma-Aldrich, 98%) was recrystallized from ethanol. *N,N*-dimethylformamide (DMF, 99.8%), ethyl 2-bromoisobutyrate (98%) (EBiB), methanol anhydrous, potassium phosphate, 2,2′-Bipyridine (bpy) were purchased from Aldrich. Anisole, *N,N*`-dicyclohexylcarbodiimide (DCC), 4-dimethylaminopyridine (DMAP) (99%) from TCI. Ethanethiol (99%), and carbon disulfide (99.9%) were purchased from Acros. Copper (I) Bromide (CuBr, Sigma-Aldrich) was purified by washing with glacial acetic acid, followed by washing with ethanol and acetone, and then dried under vacuum. 1,3,5-Trioxane (99%) were purchased from Aldrich and used as received. All other chemicals were of analytical grade and used without further purification unless otherwise stated.

2.2 Characterization

The apparent molecular weight and molecular weight distributions were measured by gel permeation chromatography (GPC, Agilent Technologies 1200 series) using a poly(methyl methacrylate) (PMMA) standard with DMF with 0.01 M LiCl was applied as the eluent at 30 °C at a flow rate of 1.00 mL/min. ^{1}H NMR spectra of the monomer and polymer were collected in DMSO-d_6 and $CDCl_3$ on a Bruker Avance 300 MHz NMR spectrometer. Ultraviolet-visible (UV–Vis) spectra were recorded using a Varian Cary-100 UV-Vis spectrophotometer equipped with a digital temperature controller. A 650 nm wavelength was used to determine LCSTs. The temperature range was from 20 to 90 ^oC with a heating and cooling rate of 1 ^oC/min. The hydrodynamic diameters were measured by dynamic light scattering (DLS) instrument (Nano ZS, Malvern, UK) using Zetasizer software 7.01. Average size and count rate were calculated from the three replicate measurements and reported as mean diameter ± standard deviation.

2.3 Synthesis

2.3.1 Synthesis of 2-(((Ethylthio)carbonothioyl)thio)-2-methylpropanoic Acid (EMP) were prepared as previously reported.[46]

2.3.2 $PHEMA_{500}$ was prepared by according to the following general procedure. A clean and dry 25ml Schlenk flask was charged with HEMA (10 mL, 82.45 mmol), bpy (25.75 mg, 0.164 mmol), methanol (7 mL), anisole (3 mL), EBiB (12.1 μL, 0.08245 mmol). The flask was deoxygenated by five freeze-pump-thaw cycles. During the final cycle, the flask was filled with argon and CuBr (11.8 mg, 0.08245 mmol) was quickly added to the frozen mixture. The flask was filled with argon and the polymerization was contucted at room temperature (RT). 6 h later, polymerization was stopped by exposing the solution to air. The resulting solution was diluted with methanol and passed through neutral alumina to remove the copper complex, and the polymer was precipitated twice in diethyl ether and dried under vacuum at room temperature for 24 h. $M_{n,GPC}$ = 195500 g/mol, M_w/M_n = 1.29 determined by GPC using DMF as eluent and linear PMMA standards. ^1H NMR (300 MHz, DMSO-d_6, δ in ppm) was as follows: 4.82 (1H, s, CH_2OH); 3.89 (2H, s, O-CH_2-CH_2); 3.58 (2H, s, O-CH_2-CH_2); 2.0-1.8 (2H, d, CH_2-C(CH_3)); 1.1-0.94 (3H, d, CH_2-C(CH_3)).

2.3.3 $PHEMA_{500}$–EMP (Macro-CTA) $PHEMA_{500}$ (0.7734 g, 5.94 mmol per HEMA repeating unit), EMP (2g, 8.91 mmol) and 4-dimethylaminopyridine (DMAP, 72.6 mg, 0.59 mmol) were added sequentially into a 50 ml round-bottomed flask containing 20 ml of DMF. The reaction flask was placed into ice-water bath for 30 min and DCC (1.84 g, 8.91 mmol) in 5 ml of DMF was then added drop-wise. The reaction was stirred for 1 h in the ice bath then the reaction mixture was allowed to stir 24 h at room temperature. During this period, the reaction mixture slowly turned brown and insoluble DCC urea precipitated out. After filtration to remove the solid, the polymer product was diluted with dichloromethane, the polymer was precipitated into hexanes three times to remove any excess DCC and DCC urea. Polymer was separated and then dried under high vacuum at RT for overnight. $M_{n,GPC}$ = 72,300 and M_w/M_n = 1.42 determined by GPC using DMF as eluent and linear PMMA standards. Successful synthesis of macro-CTA was confirmed by using ^1H NMR (300 MHz, $CDCl_3$, δ in ppm) was as follows: 4.3-4.14 (4H, d, -O-CH_2- CH_2-O-), 3.3-3.2 (2H, q, S-CH_2-CH_3), 1.95-1.50 (6H, m, O-(C=O)-C(CH_3)$_2$), 1.34-1.25 (3H, t, S-CH_2-CH_3).

2.3.4 General Procedure for the Preparation of PDMA Bottlebrushes Reversible addition-fragmentation chain transfer polymerization (RAFT) was used to synthesize the bottlebrush polymers. DMA (12 ml, 116.45 mmol), macro-CTA (0.196 g, 0.5823 mmol), AIBN (9.6 mg, 0.05823 mmol), 1,3,5-trioxane (0.3 g, 3.33 mmol, internal standard), and toluene (20 mL) were sealed in a 50 mL Schlenk flask equipped with a magnetic stir bar. The reaction mixture was purged with argon for 30 min, and the reaction flask was placed in a preheated oil bath at 40 ^{o}C. Samples were taken periodically by syringe to determine the molecular weight and PDI by GPC and monomer conversion by ^{1}H NMR spectroscopy. The polymerization was stopped by cooling the flask at room temperature and exposing the solution to air. The solution was concentrated and the polymer was precipitated into cold diethyl ether. The polymer was redisolved in dichloromethane, and reprecipitated into cold diethyl ether three times and dried under vacuum at room temperature for 24 h.

2.3.5 General Procedure for the Preparation of Linear PDMA

DMA (16 ml, 155.3 mmol), EMP (0.174 g, 0.776 mmol), AIBN (3.2 mg, 0.0194 mmol), 1,3,5-trioxane (0.3 g, 3.33 mmol, internal standard) were added to a 50 mL Schlenk flask with 20ml DMF. The reaction mixture was purged with argon for 30 min, and the reaction flask was contucted in a preheated oil bath at 50 ^{o}C. The samples were removed periodically by syringe to determine the molecular weight and PDI by GPC and monomer conversion by ^{1}H NMR spectroscopy. The reaction was stopped by cooling the flask at room temperature and opening the flask to air.

3. Results and Discussion

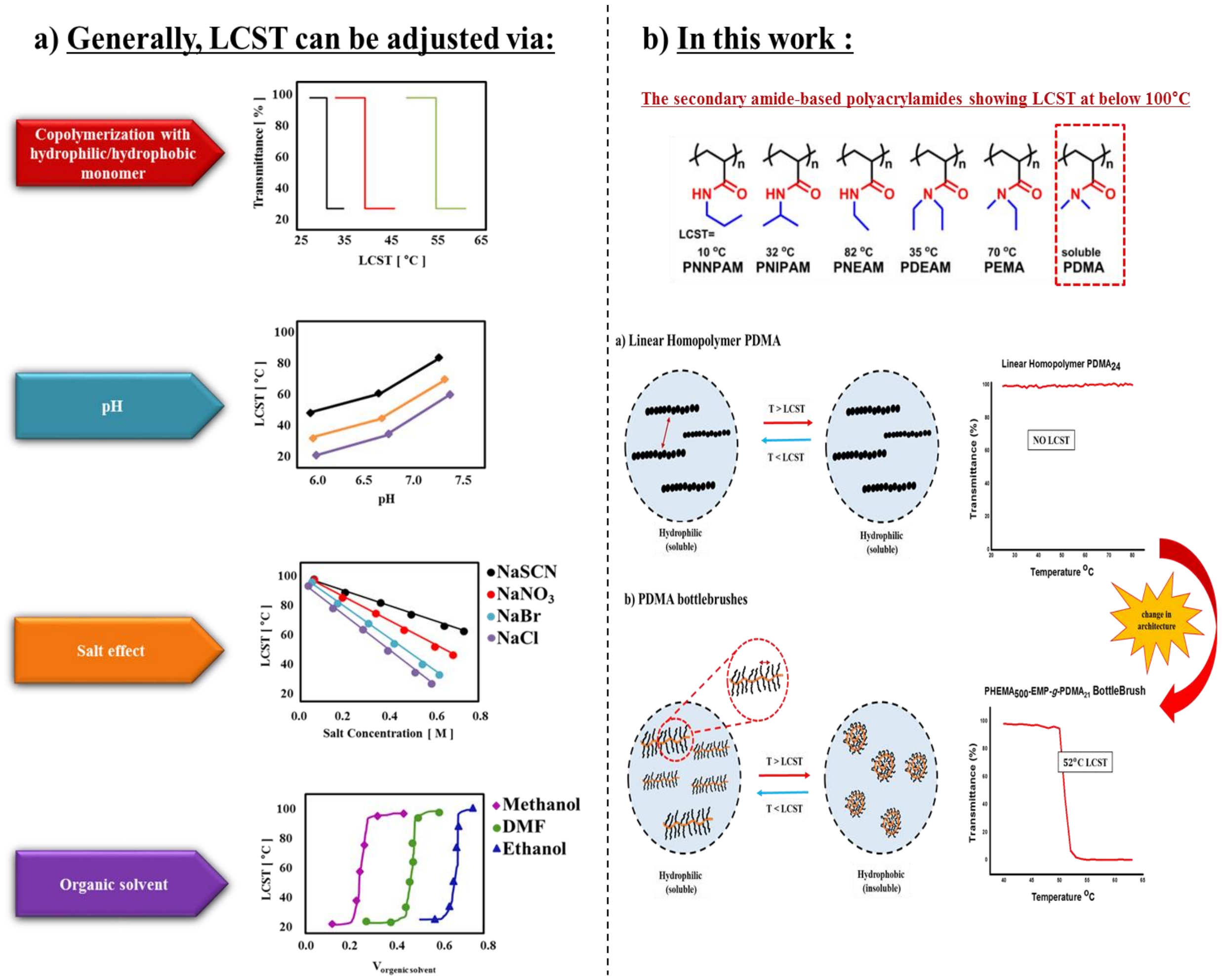

Scheme 1. Schematic illustration of the effect of change in the architecture of PDMA on LCST.

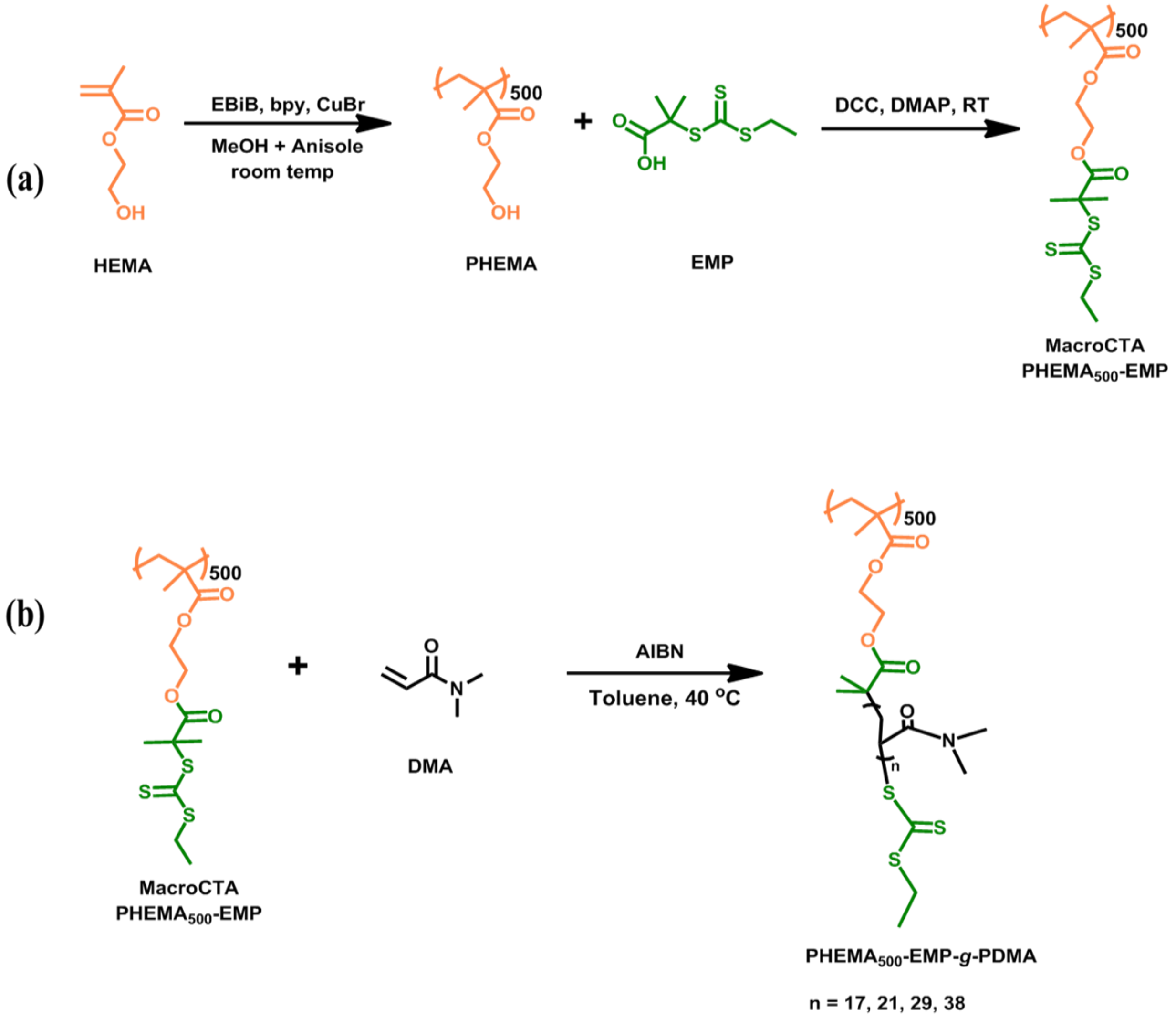

Scheme 2. Synthesis of PHEMA$_{500}$ and subsequent Macro-CTA backbones (a), and the synthesis of bottle brushes with PDMA side chains grown from a Macro-CTA backbone by RAFT polymerization (b).

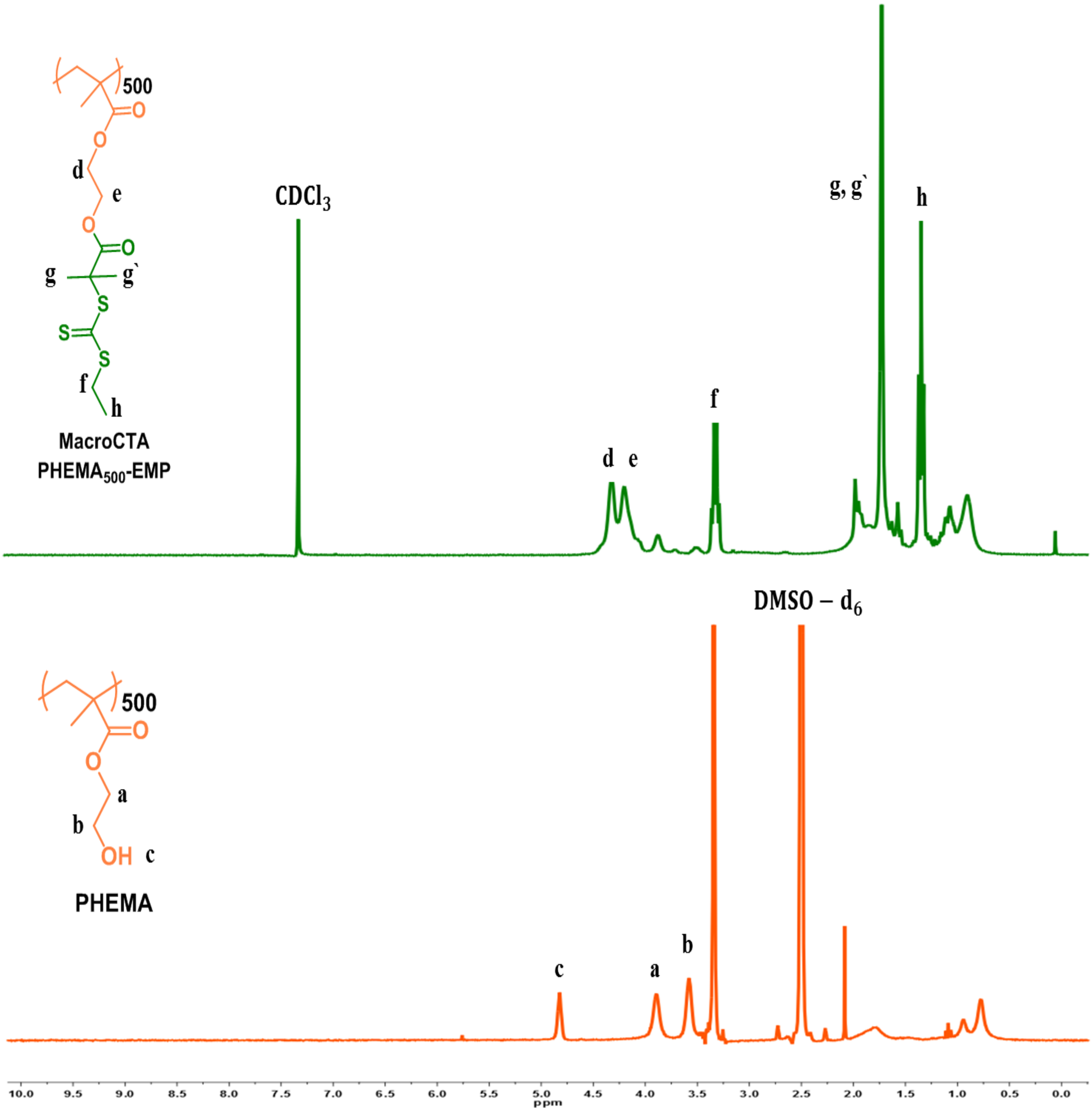

Figure 1. ^{1}H NMR spectrum of PHEMA$_{500}$ in DMSO-d$_6$ and PHEMA$_{500}$-EMP macro-CTA (backbone) in CDCl$_3$.

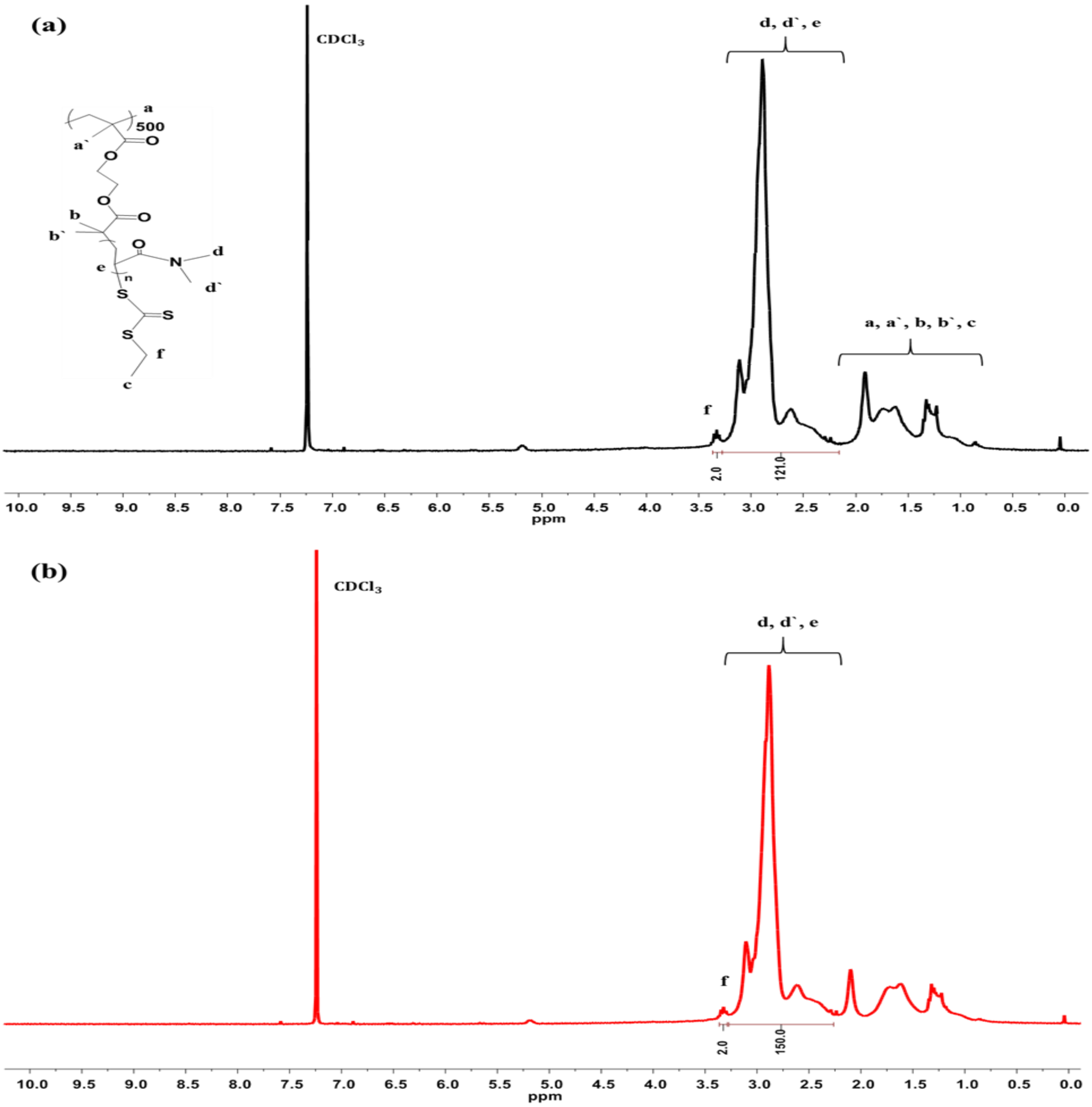

Figure 2. ^{1}H NMR spectrum of PHEMA$_{500}$-EMP-*g*-PDMA$_{17}$ (a), and PHEMA$_{500}$-EMP-*g*-PDMA$_{21}$ (b) in CDCl$_3$.

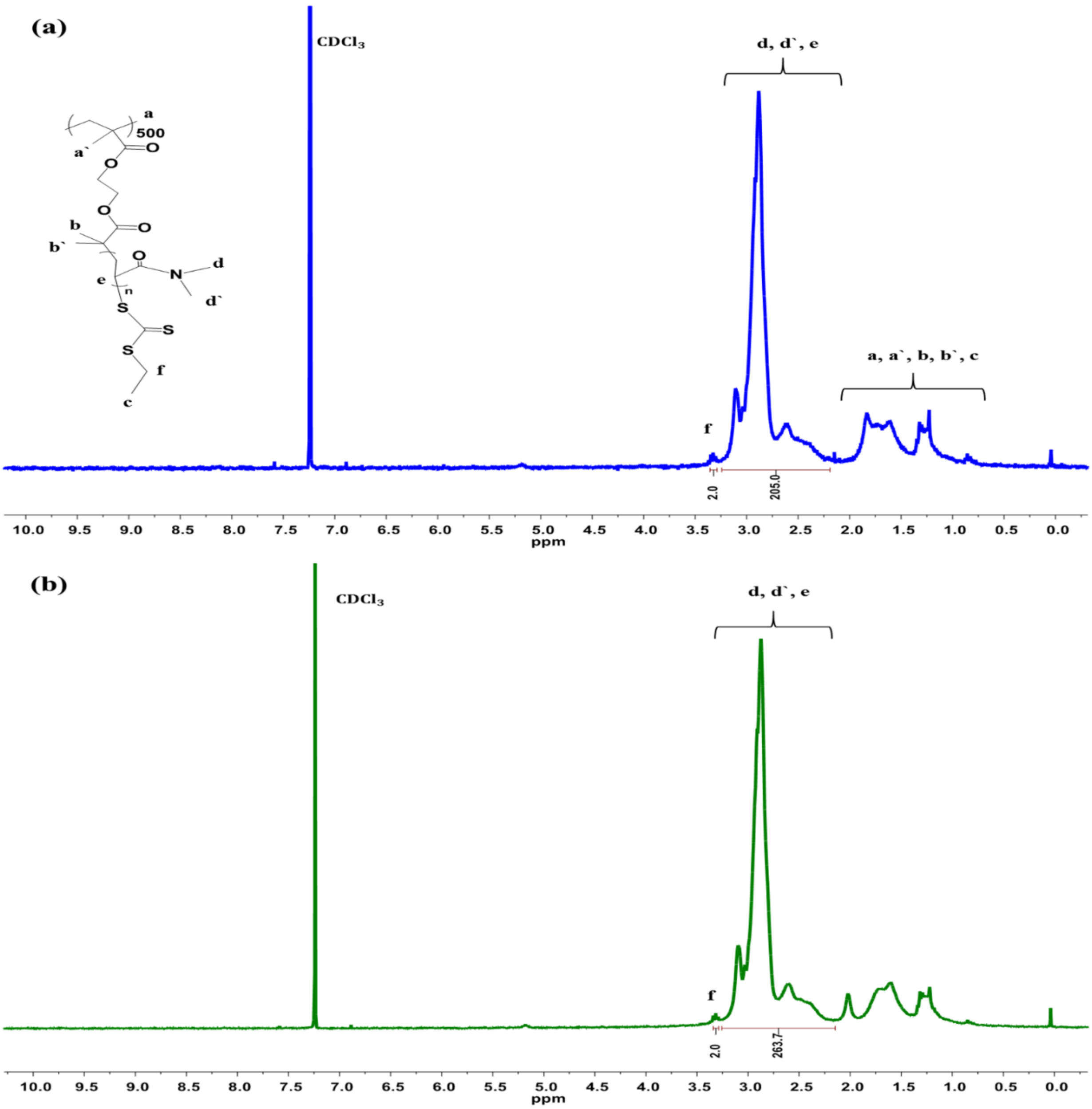

Figure 3. ^{1}H NMR spectrum of PHEMA$_{500}$-EMP-*g*-PDMA$_{29}$ (a), and PHEMA$_{500}$–EMP -*g*-PDMA$_{38}$ (b) in CDCl$_3$.

The synthesis of PDMA bottlebrush polymers are schematically illustrated in Scheme 2. $PHEMA_{500}$ was prepared via atom transfer radical polymerization (ATRP) as a precursor of the brush backbone. A CuBr/bpy as a catalyst system was used for the ATRP of HEMA using ethyl 2-bromoisobutyrate (EBiB) as an initiator. ATRP polymerization, the ratio of [HEMA]:[EBiB]:[CuBr]:[bpy] was fixed at 1000:1:1:2 and a mixed solvent system of anisole/methanol (2/1 by volume ratio) was employed to ensure a homogeneous reaction mixture throughout the HEMA polymerization. The molecular weight and molecular weight distribution of the resulting PHEMA were determined using a GPC DMF line with polymethyl methacrylate (PMMA) standards (M_n = 195 500 g/mol, M_w/M_n = 1.29). The successful synthesis of $PHEMA_{500}$ was confirmed by ^{1}H NMR spectroscopy (Figure 1).

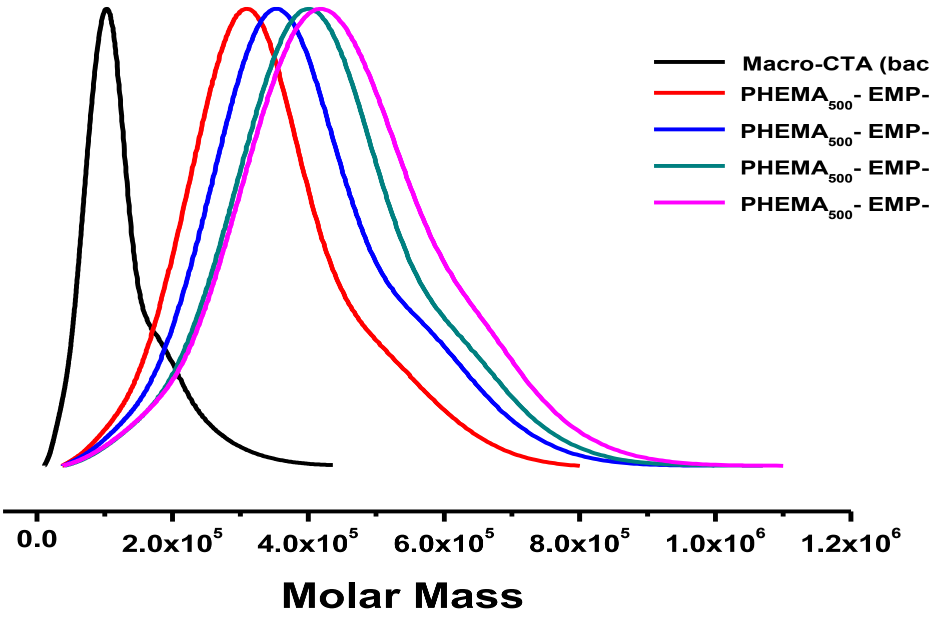

Figure 4. GPC traces of $PHEMA_{500}$-EMP macro-CTA and a series of $PHEMA_{500}$-EMP-*g*-PDMA bottlebrushes measured by using linear PMMA standards.

The EMP was selected as an efficient chain transfer agent CTA. In the next step, the -OH groups of $PHEMA_{500}$ were reacted with EMP to yield $PHEMA_{500}$-EMP as a macro-CTA in the presence of dicyclohexylcarbodiimide (DCC) as a coupling agent. The resulting $PHEMA_{500}$-EMP was analyzed by GPC using DMF LiCl line (M_n = 78 500 g/mol, M_w/M_n = 1.3) (Figure 4). The ^{1}H NMR spectra provided evidence of the successful synthesis of macro-CTA. As shown in

Figure 1, the transformation of PHEMA into PHEMA$_{500}$-EMP by monitoring the disappearance of the peak of (c) of a PHEMA hydroxyl group peak at 4.82 ppm after esterification.

Table 1. Properties of synthesized macro-CTA backbone and series of PHEMA$_{500}$-EMP-*g*-PDMA bottlebrushes.

Polymer [a]	**Conv**[b] **(%)**	**$M_{n,\ theory}$**[c] **(g/mol)**	**$M_{n,\ ^1H\ NMR}$**[d] **(g/mol)**	**$M_{n,\ app}$**[e] **(g/mol)**	**PDI**[e]	**LCST**[f] **(°C)**
PHEMA$_{500}$-EMP		65300	52300	78500	1.3	
PHEMA$_{500}$-EMP-g-PDMA$_{17}$	10	67300	54000	244000	1.21	31
PHEMA$_{500}$-EMP-g-PDMA$_{21}$	12.5	67800	54400	279000	1.22	52
PHEMA$_{500}$-EMP-g-PDMA$_{29}$	15	68300	55200	286100	1.28	72
PHEMA$_{500}$-EMP-g-PDMA$_{38}$	20	69300	56070	322000	1.22	soluble

a) Experimental degree of polymerization (DP) determined by 1H NMR spectroscopy is given as a subscript; b) Determined by ^{1}H NMR spectroscopy; c) Theoretical molecular weight determined from monomer conversions; d) Experimental molecular weights calculated from ^{1}H NMR spectroscopy; e) Apparent number-average molecular weight and PDI determined by GPC using a PMMA calibration, DMF with 0.01M LiCl as the eluent; f) Lower critical solution temperature (LCST) as determined by turbidimetry using UV-Vis spectroscopy.

Synthesis of PHEMA$_{500}$-EMP-*g*-PDMA bottlebrush polymers, PDMA side chains were grown from PHEMA$_{500}$-EMP macro-CTA by RAFT in the presence of AIBN. Polymerization of bottlebrush conditions were used for the side chain synthesis: [DMA] : [Macro-CTA] : [AIBN] : [trioxane] = 200:1:0.1:5 for the synthesis of series of PHEMA$_{500}$-EMP-*g*-PDMA. 1,3,5-trioxane was used as an internal standard at 40 ^oC. The concentration of AIBN was studied by selecting Macro-CTA : AIBN ratios of 1:0.1. The reaction temperature was only 40 ^oC for the system in order to decompose AIBN very slowly.

Samples were taken from the reaction mixture by syringe at regularly spaced intervals during polymerization to obtain the PDMA with different side chain lengths as well as to monitor conversion and molecular weight evolution. Monomer conversions by ^{1}H NMR spectroscopy in DMSO-d_6 by comparing the integration area of the vinyl protons of DMA and OCH_2 protons of the 1,3,5-trioxane internal standard.

The resulting PHEMA$_{500}$-EMP-*g*-PDMA bottlebrush polymers were analyzed by GPC using DMF with LiCl and ^{1}H NMR spectroscopy using $CDCl_3$ as the solvent. ^{1}H NMR spectroscopy was used to calculate the final incorporation ratio of the DMA, and Macro-CTA by comparing the relative integral area of the signals from (f) of -SCH_2 group peak of Macro-CTA at 3.3-3.2 ppm, (e) of -CHCO group peak and (d, d) dimethyl protons of DMA at 3.2-2.25 ppm (Figure 2 and Figure 3). The GPC traces of the bottlebrush polymer clearly shifted to the higher molecular region with increasing side chain length is observed, which is qualitatively indicative of the molecular weight increasing throughout the side chain length, as shown in Figure 4. Also, the molecular weight distribution was relatively low, indicating good controlled growth of the side chain from macro-CTA. Results from the various side chain length of bottlebrush polymers are summarized in Table 1. Moreover, the apparent molecular weights of all bottlebrush polymers obtained by GPC were higher than the theoretical molecular weight calculated from the DMA conversion due to the difference in hydrodynamic volumes of PDMA and PMMA standards. However, the theoretical molecular weights were relatively close to NMR molecular weights.

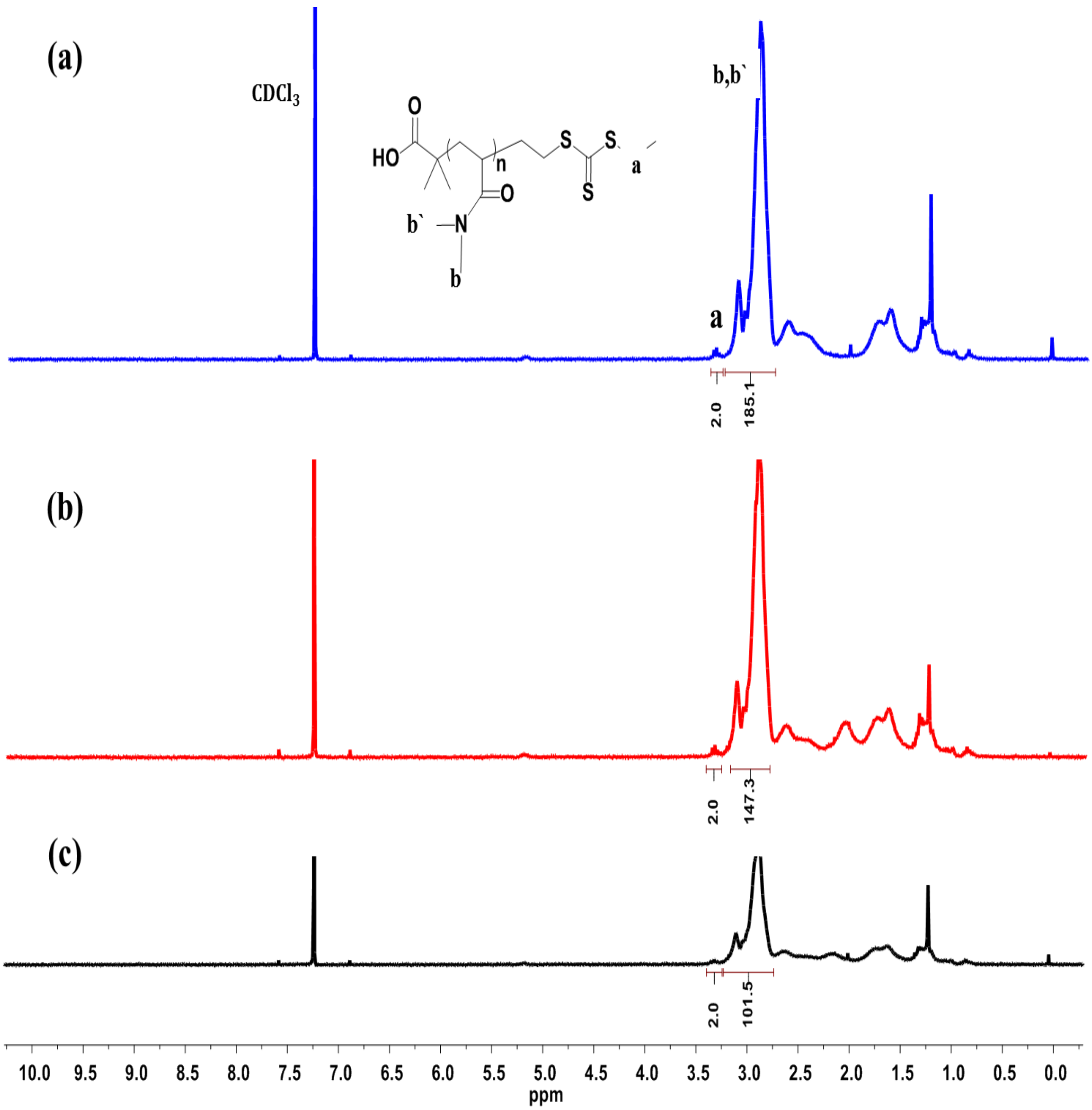

Figure 5. ^{1}H NMR spectrum of linear homopolymers, PDMA$_{30}$ (a), and PDMA$_{24}$ (b), and PDMA$_{17}$ (c) in CDCl$_3$.

Linear PDMA homopolymers were synthesized via reversible addition-fragmentation chain transfer (RAFT) polymerization. The polymerization condition was fixed at [DMA] : [EMP] : [AIBN] : [trioxane] = 200:1:0.025:5 for the synthesis of series of linear PDMA homopolymer. 1,3,5-trioxane was used as an internal standard at 50 °C. The successful synthesis of series of linear PDMA homopolymer were confirmed by ^{1}H NMR spectroscopy (Figure 5). Furthermore, the resulting series of linear PDMA homopolymers were synthesized as the same degree of polymerization (DP) of PDMA bottlebrush polymers.

As in the literature, the lower critical solution temperature (LCST) of PDMA was determined to be above 100 °C which are around 200 °C. This LCST of PDMA is the highest phase-transition temperature among all poly(*N,N*-dialkylacrylamides)s. PDMA bottlebrushes studied in this work, we focused on the effect of the change in architecture on LCST, which is by using the polymer-polymer interaction that is one of the significant properties of the bottlebrush polymer, as shown in Scheme 1b. More specifically, these studies showed that the PDMA bottlebrushes exhibited LCST below 100 °C with increasing polymer-polymer interaction on side chains and the effect of entropy of side chains of bottlebrushes. The transmittance of aqueous solutions of PDMA bottlebrushes were measured using a UV spectrometer in order to determine the effect of side chain length on LCST behavior. The transmittance of 1 wt % aqueous solution of the bottlebrush polymer was monitored at 650 nm at a heating or cooling rate of 1.0 °C min $^{-1}$. LCST study temperature range was from 20 to 90 °C. UV-vis measurements shown in Figure 6, the containing shorter side chain length PHEMA500-EMP-*g*-PDMA$_{17}$ exhibited an LCST near 31 °C. The LCST of PHEMA500-EMP-*g*-PDMA$_{21}$, PHEMA500-EMP-*g*-PDMA$_{29}$ exhibited at 52 and 72 °C, respectively. Note that the LCST values can be affected by side chain stretching and side chain length of bottlebrushes.

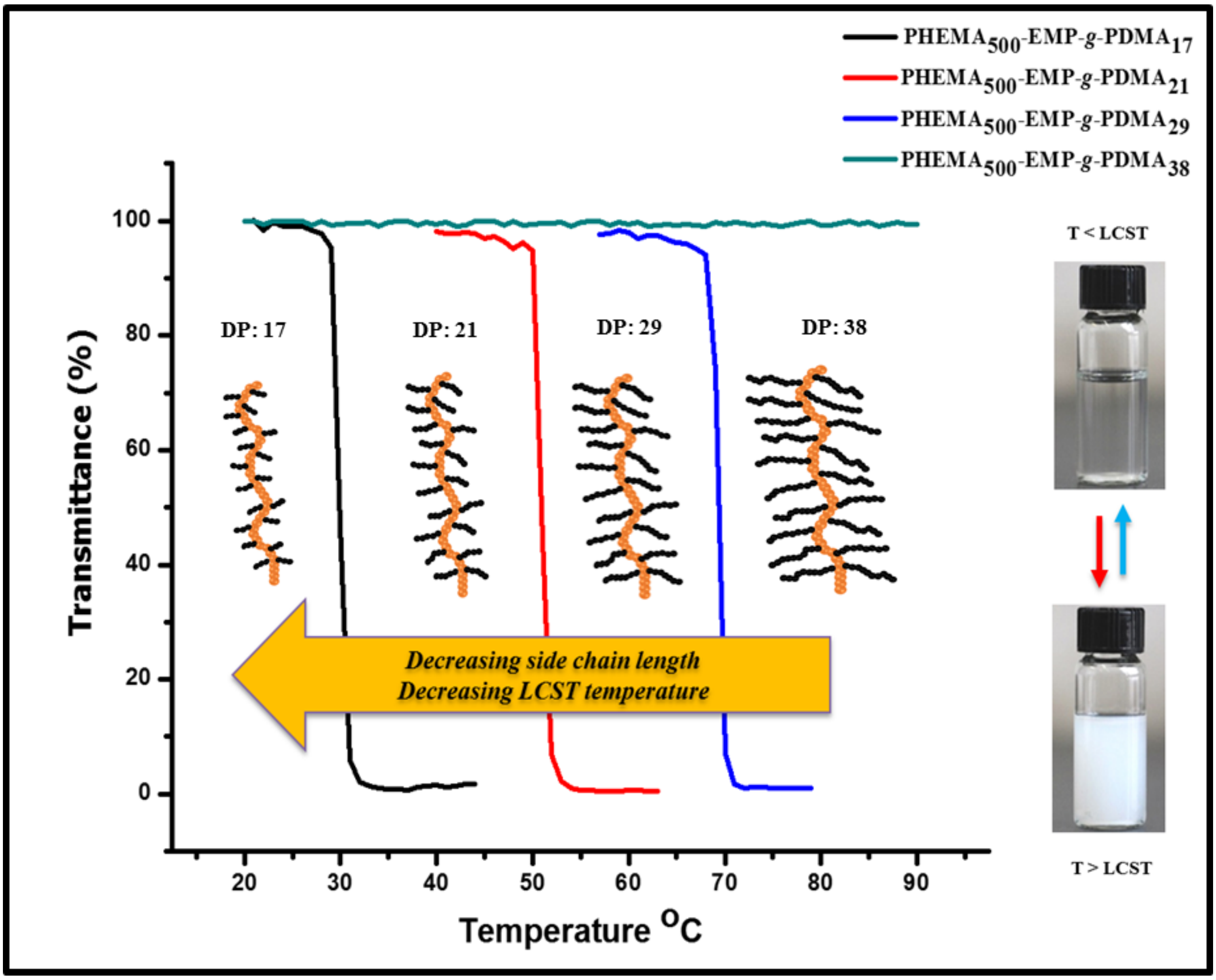

Figure 6. UV-vis transmittance spectra for effect of the side chain length on the temperature dependence of optical transmittance changes at 650 nm for 1% aqueous solution of $PHEMA_{500}$-EMP-g-PDMA bottlebrush polymer.

As expected, decreasing the side chain length of PDMA bottlebrushes decreases LCST (Figure 6). According to UV-vis transmittance results, when increasing side chain length by a difference of 10, there is showing 20 ^{o}C increases in each LCST. Therefore, containing the longest side chain length PHEMA$_{500}$-EMP-*g*-PDMA$_{38}$ did not show an apparent thermal transition up to 90 °C. Above the DP 30, solution of PDMA brush polymer can not appear LCST at below 100 °C due to hydrophilicity is strong in the PDMA side chain. Interestingly, increasing side chain length increases the flexibility of side chains, and the distance between the side chains decreases. Hence, above 100 °C is required to break the polymer-water interaction between the side chains. Therefore, above DP 40 of PDMA bottlebrush is exhibited behavior of soluble due to the entropy of side chains are positive (Figure 6). We have also compared the thermoresponsive behavior of linear and bottlebrush PDMAs with the same chain length. According to the results of the UV-vis, for the series of linear PDMA can not appear LCST below 100 °C (Figure 7a). This could be due to the dissolved linear polymers in free form in aqueous media, polymer-water interaction increases than polymer-polymer interaction and the hydrophilic forces in PDMA are greatest. In addition, the distance between the linear polymers being long causes the soluble behavior when the entropy to be positive and enthalpy to be negative. Hereby, above 100 °C is required to break the polymer-water H bonding between the polymers.

In contrast to Linear PDMA, the series of bottlebrush PDMA in aqueous media appear LCST below 100 °C (Figure 7b). The physically significant difference between brush polymers and linear polymers is that the bottle brush architecture consists of a linear backbone with tailored linear side chains. Therefore, the dissolved bottlebrush polymers in the aqueous media, increasing polymer-polymer interaction due to architecture of bottlebrush, and polymer-water interaction of bottlebrushes is less than linear PDMA. When increasing temperature cause the hydrophobic forces in brush PDMA are rising and aggregation between side chains begins. More specifically, the distance between side chains being short causes the LCST behavior when the entropy to be negative and enthalpy to be negative.

All of the PDMA bottlebrushes were measured by dynamic light scattering (DLS) to determine the hydrodynamic and count rate values in heating/cooling. The hydrodynamic and count rate values were monitored at 0.1 wt % aqueous solution in the temperature range of 25–70 °C with a step-size of 1 K for both heating and cooling. After changing the temperature, the sample was equilibrated for 2min and then measured three times. Each reported value was an average of 12 runs. The results are reported in Figure 8. It can be clearly seen that the hydrodynamic size increased for the brush samples in increasing temperature. The aggregates formed upon heating for all bottlebrushes were small but did not immediately deaggregate upon cooling (Figure 8). Note that by raising the temperature of a homogeneous solution, phase separation will occur accompanied by an endothermic heat effect. Interestingly, as seen in Figure 8, the reason for the hydrodynamic and count rate values of all PDMA bottlebrush solutions to form irregular curves, after cooling the remixing exotherm is somewhat smaller than the demixing, it causes indicates that the remixing of the PDMA brush solutions is slower than the demixing of these systems.

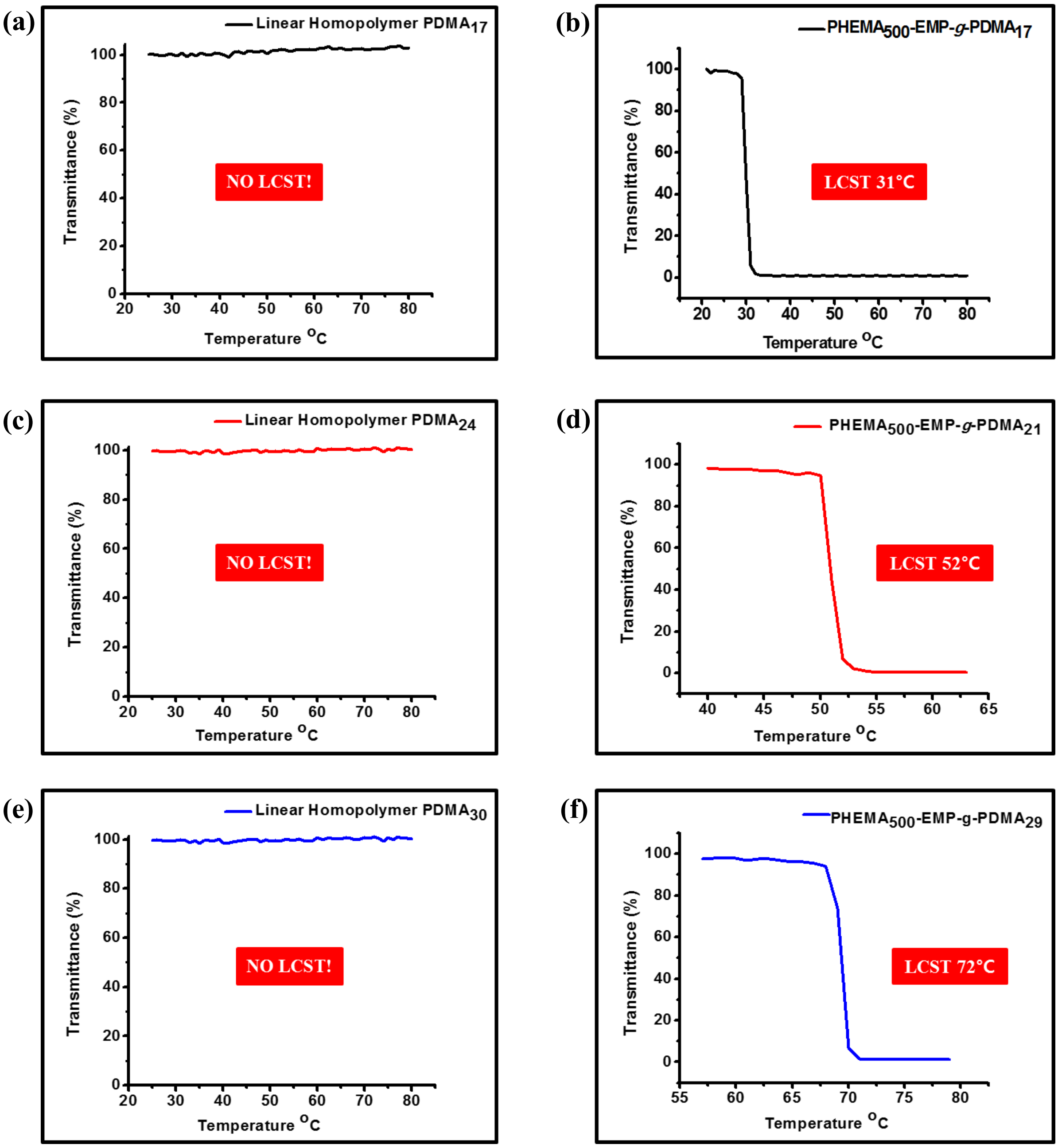

Figure 7. Effect of the architecture on the temperature dependence of optical transmittance changes at 650 nm for homopolymer and bottlebrush polymer DMA aqueous solution.

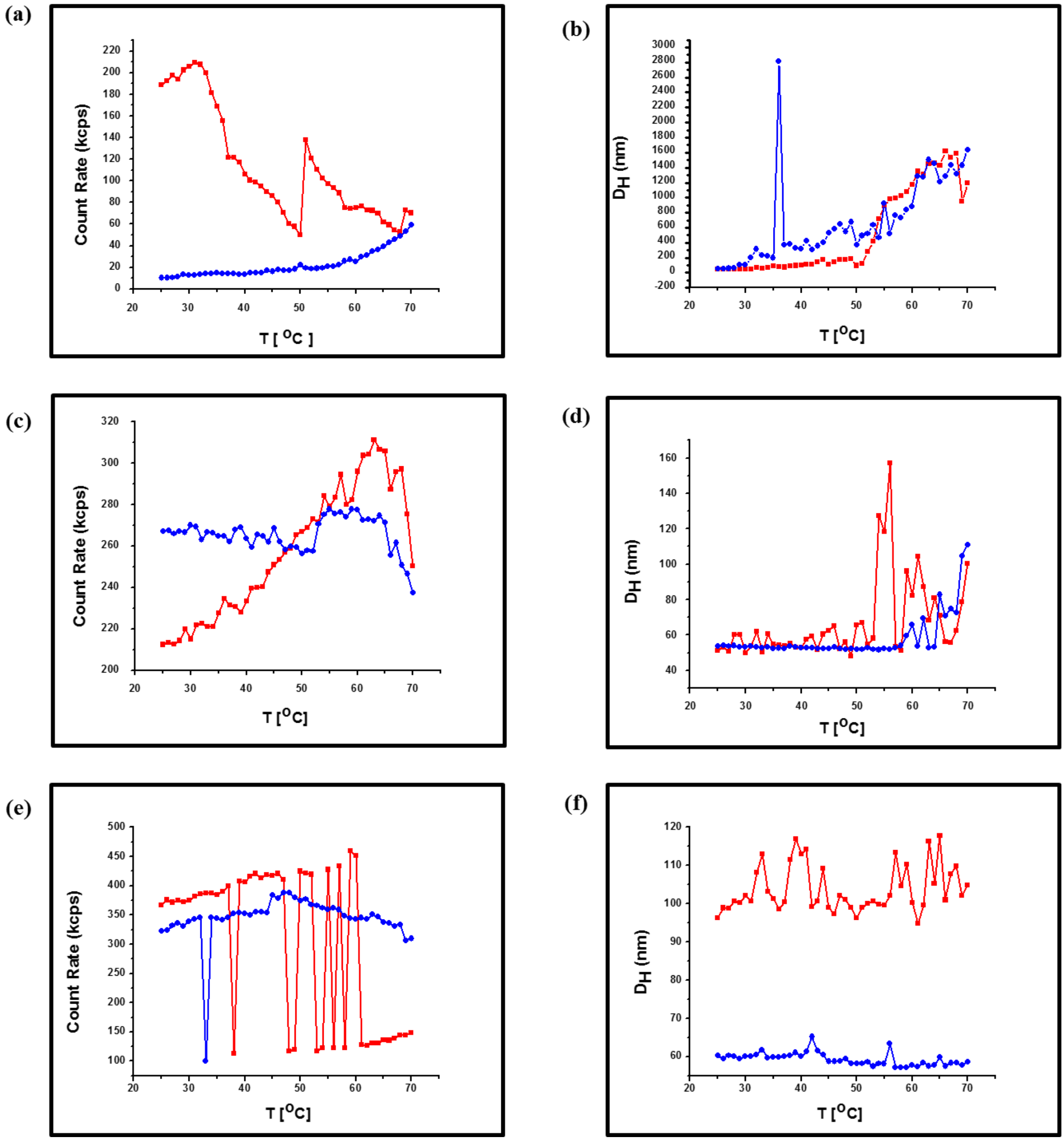

Figure 8. Temperature-cycled dynamic light scattering (DLS) for bottlebrush polymer at 0.1 wt.-% solutions concentrations, PHEMA$_{500}$-EMP-*g*-PDMA$_{17}$: (a,b); PHEMA$_{500}$-EMP-g-PDMA$_{21}$: (c,d); and PHEMA$_{500}$-EMP-g-PDMA$_{29}$: (e,f). **Left**: count rate vs. temperature, **right**: hydrodynamic diameter (DH) vs. temperature, heating curve (red squares), cooling curve (blue circles).

4. Conclusion

Well-defined water-soluble PDMA bottlebrushes were synthesized with PDMA side chains growing from macro-CTA by the “grafting from” approach using RAFT polymerization techniques for the effect of the change in the polymer architecture on the LCST value of the PDMA. The synthesized bottlebrushes were of high molecular weight and relatively low polydispersities. Herein, unlike the methods in the literature, the effect of the change in polymer architecture on PDMA which does not show LCST below 100 °C was proven by comparing it using UV-vis with the linear homopolymer PDMA synthesized at the same DP with PDMA bottlebrush polymers. PDMA bottlebrushes with different side chain lengths showed an LCST below 100. In the bottlebrush polymer, the polymer-polymer interaction is increased due to the close distance of the side chains causes the entropy of the polymer brushes to become negative at LCST. The LCST values of series of bottlebrush decreased when decreasing PDMA side chain length on bottlebrush.

References

1. Beers, K. L.; Gaynor, S. G.; Matyjaszewski, K.; Sheiko, S. S.; Möller, M., The synthesis of densely grafted copolymers by atom transfer radical polymerization. *Macromolecules* **1998,** *31* (26), 9413-9415.

2. Xia, Y.; Olsen, B. D.; Kornfield, J. A.; Grubbs, R. H., Efficient synthesis of narrowly dispersed brush copolymers and study of their assemblies: The importance of side chain arrangement. *JACS* **2009,** *131* (51), 18525-18532.

3. Sveinbjörnsson, B. R.; Weitekamp, R. A.; Miyake, G. M.; Xia, Y.; Atwater, H. A.; Grubbs, R. H., Rapid self-assembly of brush block copolymers to photonic crystals. *Proceedings of the National Academy of Sciences* **2012,** *109* (36), 14332-14336.

4. Verduzco, R.; Li, X.; Pesek, S. L.; Stein, G. E., Structure, function, self-assembly, and applications of bottlebrush copolymers. *Chemical Society Reviews* **2015,** *44* (8), 2405-2420.

5. Onbulak, S.; Rzayev, J., Synthesis and one-dimensional assembly of cylindrical polymer nanoparticles prepared from tricomponent bottlebrush copolymers. *Journal of Polymer Science Part A: Polymer Chemistry* **2017,** *55* (23), 3868-3874.

6. Vatankhah-Varnosfaderani, M.; Daniel, W. F.; Everhart, M. H.; Pandya, A. A.; Liang, H.; Matyjaszewski, K.; Dobrynin, A. V.; Sheiko, S. S., Mimicking biological stress–strain behaviour with synthetic elastomers. *Nature* **2017,** *549* (7673), 497-501.

7. López-Barrón, C. R.; Brant, P.; Eberle, A. P.; Crowther, D. J., Linear rheology and structure of molecular bottlebrushes with short side chains. *Journal of Rheology* **2015,** *59* (3), 865-883.

8. Dalsin, S. J.; Hillmyer, M. A.; Bates, F. S., Linear rheology of polyolefin-based bottlebrush polymers. *Macromolecules* **2015,** *48* (13), 4680-4691.

9. Haugan, I. N.; Maher, M. J.; Chang, A. B.; Lin, T.-P.; Grubbs, R. H.; Hillmyer, M. A.; Bates, F. S., Consequences of grafting density on the linear viscoelastic behavior of graft polymers. *ACS Macro Letters* **2018,** *7* (5), 525-530.

10. Dalsin, S. J.; Hillmyer, M. A.; Bates, F. S., Molecular weight dependence of zero-shear viscosity in atactic polypropylene bottlebrush polymers. *ACS Macro Letters* **2014,** *3* (5), 423-427.

11. Bak, J. M.; Jha, G.; Ahn, E.; Jung, S.-H.; Jeong, H. M.; Kim, B.-S.; Lee, H.-i. Molecular brushes with extreme grafted side chain densities. *Polymer* **2012**, *53*, 3462-3468.

12. Rathgeber, S.; Lee, H.-i.; Matyjaszewski, K.; Di Cola, E. Rheooscillations of a bottlebrush polymer solution due to shear-induced phase transitions between a shear molten state and a line hexatic phase. *Macromolecules* **2007**, *40*, 7680-7688.

13. Strandman, S.; Zhu, X. Thermo-responsive block copolymers with multiple phase transition temperatures in aqueous solutions. *Progress in Polymer Science* **2015**, *42*, 154-176.

14. Smith, A. E.; Xu, X.; McCormick, C. L. Stimuli-responsive amphiphilic (co) polymers via RAFT polymerization. *Progress in polymer science* **2010**, *35*, 45-93.

15. Schattling, P.; Jochum, F. D.; Theato, P. Multi-stimuli responsive polymers–the all-in-one talents. *Polymer Chemistry* **2014**, *5*, 25-36.

16. Roy, D.; Brooks, W. L.; Sumerlin, B. S. New directions in thermoresponsive polymers. *Chemical Society Reviews* **2013**, *42*, 7214-7243.

17. Halperin, A.; Kröger, M.; Winnik, F. M. Poly (N-isopropylacrylamide) phase diagrams: fifty years of research. *Angewandte Chemie International Edition* **2015**, *54*, 15342-15367.

18. Heskins, M.; Guillet, J. E. Solution properties of poly (N-isopropylacrylamide). *Journal of Macromolecular Science—Chemistry* **1968**, *2*, 1441-1455.

19. Ono, Y.; Shikata, T. Hydration and dynamic behavior of poly (N-isopropylacrylamide) s in aqueous solution: a sharp phase transition at the lower critical solution temperature. *Journal of the American Chemical Society* **2006**, *128*, 10030-10031.

20. Okada, Y.; Tanaka, F. Cooperative hydration, chain collapse, and flat LCST behavior in aqueous poly (N-isopropylacrylamide) solutions. *Macromolecules* **2005**, *38*, 4465-4471.

21. Wang, X.; Qiu, X.; Wu, C. Comparison of the coil-to-globule and the globule-to-coil transitions of a single poly (N-isopropylacrylamide) homopolymer chain in water. *Macromolecules* **1998**, *31*, 2972-2976.

22. Costa, R. O.; Freitas, R. F. Phase behavior of poly (N-isopropylacrylamide) in binary aqueous solutions. *Polymer* **2002**, *43*, 5879-5885.

23. Cho, E. C.; Lee, J.; Cho, K. Role of bound water and hydrophobic interaction in phase transition of poly (N-isopropylacrylamide) aqueous solution. *Macromolecules* **2003**, *36*, 9929-9934.

24. Y. M. Kyong, S. Y. Kiel, C. S. Cho and Y. M. Lee, Polym. J., 1997, 38, 2759–2765.

25. El-Ejmi AAS and Huglin MB, PolymInt 39:113–119 (1996).

26. El-Ejmi AAS and Huglin MB, Eur Polym 33:1281–1284 (1997).

27. Barker IC, Cowie JMG,Huckerby TN, Shaw DA, Soutar I and Swanson L, Macromolecules

36:7765–7770 (2003).

28. Ranganathan K, Deng R, Kainthan RK, Wu C, Brooks DE and Kizhakkedathu JN, Macromolecules 41:4226–4234 (2008).

29. Liu HY and Zhu XX, Polymer 40:6985–6990 (1999).

30. Feil, H.; Bae, Y.; Feijen, J.; Kim, S. W. Mutual influence of pH and temperature on the swelling of ionizable and thermosensitive hydrogels. *Macromolecules* **1992**, *25*, 5528-5530.

31. Brazel, C. S.; Peppas, N. A. Synthesis and Characterization of Thermo-and Chemomechanically Responsive Poly (N-isopropylacrylamide-co-methacrylic acid) Hydrogels. *Macromolecules* **1995**, *28*, 8016-8020.

32. Zhou, S.; Chu, B. Synthesis and volume phase transition of poly (methacrylic acid-co-N-isopropylacrylamide) microgel particles in water. *The Journal of Physical Chemistry B* **1998**, *102*, 1364-1371.

33. Determan, M. D.; Cox, J. P.; Seifert, S.; Thiyagarajan, P.; Mallapragada, S. K. Synthesis and characterization of temperature and pH-responsive pentablock copolymers. *Polymer* **2005**, *46*, 6933-6946.

34. Van Durme, K.; Rahier, H.; Van Mele, B. Influence of additives on the thermoresponsive behavior of polymers in aqueous solution. *Macromolecules* **2005**, *38*, 10155-10163.

35. McPhee, W.; Tam, K. C.; Pelton, R. Poly (N-isopropylacrylamide) latices prepared with sodium dodecyl sulfate. *Journal of colloid and interface science* **1993**, *156*, 24-30.

36. He, C.; Zhao, C.; Chen, X.; Guo, Z.; Zhuang, X.; Jing, X. Novel pH-and temperature-responsive block copolymers with tunable pH-responsive range. *Macromolecular rapid communications* **2008**, *29*, 490-497.

37. Tanaka, F.; Koga, T.; Kojima, H.; Xue, N.; Winnik, F. M. Preferential adsorption and co-nonsolvency of thermoresponsive polymers in mixed solvents of water/methanol. *Macromolecules* **2011**, *44*, 2978-2989.

38. Bischofberger, I.; Calzolari, D. C.; Trappe, V. Co-nonsolvency of PNiPAM at the transition between solvation mechanisms. *Soft Matter* **2014**, *10*, 8288-8295.

39. Gao H, Matyjaszewski K. J Am Chem Soc 2007;129(20):6633-9.

40. Vogt AP, Sumerlin BS. Macromolecules 2006;39(16):5286-92.

41. Neugebauer D, Zhang Y, Pakula T, Sheiko SS, Matyjaszewski K. Macromolecules 2003;36(18):6746-55.

42. Ishizu K, Tsubaki S, Uchida SJ. Macromol Sci. Pure Appl Chem 1995; A32(7):1227-34.

43. Beers KL, Gaynor SG, Matyjaszewski K, Sheiko SS, Moeller M. Macromolecules 1998;31(26):9413-5.
44. Lee H, Jakubowski W, Matyjaszewski K, Yu S, Sheiko SS. Macromolecules 2006;39(15):4983-9.
45. Lee H-i, Matyjaszewski K, Yu-Su S, Sheiko SS. Macromolecules 2008;41(16):6073-80.
46. Schmidt, B. V.; Hetzer, M.; Ritter, H.; Barner-Kowollik, C. Cyclodextrin-complexed RAFT agents for the ambient temperature aqueous living/controlled radical polymerization of acrylamido monomers. *Macromolecules* **2011**, *44*, 7220-7232.